Available online at www.sciencedirect.com
SCIENCE DIRECT®
Journal of Power Sources 146 (2005) 510–515
JOURNAL OF POWER SOURCES
www.elsevier.com/locate/jpowsour

Solid solution of nickel oxide and manganese oxide as negative active material for lithium secondary cells

Xingjiang Liu, Hideo Yasuda *, Masanori Yamachi

Corporate R&D Center, Japan Storage Battery Co. Ltd., Nishinosho, Kisshoin, Minami-ku, Kyoto 601-8520, Japan

Available online 16 June 2005

Abstract

The solid solution of nickel oxide and manganese oxide has been synthesized successfully by heating $Ni_{1-a}Mn_aOOH$ at a temperature ranging from 350 to 1000 °C in oxygen atmosphere, and investigated as a high-capacity negative active material for lithium secondary cells. The discharge capacity of nickel and manganese oxide solid solution was decreased with increasing heat-treatment temperature. The average discharge potential shifts toward negative as increasing Mn content in the solid solution. Meanwhile, large amount of Mn in the oxide solid solution caused a poor cycleability. The $Ni_{0.75}Mn_{0.25}O_{1.36}$ obtained by heating its raw material at 600 °C delivered a large discharge capacity over 700 mAh g^{-1} with a relatively low average discharge potential of 1.69 versus Li/Li^+. In addition, the $Ni_{0.75}Mn_{0.25}O_{1.36}$ gave the best capacity retention of 91% with representative charge–discharge curves even after 22 cycles. According to the results of XRD and high-resolution X-ray fluorescence spectrometer (HRXRF) measurements for the oxide solid solution before and after the first charge, it was clear that an amorphous-like or nano-sized phase was formed during the first electrochemical reduction; all of the nickel and a part of manganese were reduced to metallic state after charge to 0.2 V versus Li/Li^+.

Keywords: Nickel oxide; Manganese oxide; Solid solution; Negative active material; HRXRF; Lithium secondary cells

1. Introduction

Recently, to realize a new secondary cell with higher energy density not only for portable electronics, but also electric power tools and EV applications, a worldwide effort has been made to find alternative positive and negative active materials. The 3d-transition metal oxides, such as CoO, Co_3O_4, NiO, FeO and Cu_2O were reported as high-capacity negative active material with smaller volume change compared with lithium alloys. The mechanism of lithium reactivity differs from the classical Li insertion/deinsertion or Li-alloying/dealloying processes and involves the formation and decomposition of Li_2O, accompanying the reduction and oxidation of metal nano-particles [1–7].

$$Me_xO_y + 2yLi^+ + 2ye^- \Leftrightarrow xMe + yLi_2O \quad (1)$$

Usually, transition metal oxide delivers a capacity from 600 to 1000 mAh g^{-1} according to the reaction (1) with two or three electrons reaction at ambient temperature.

The $Li_3CuFe_3O_7$ with γ-$LiFeO_2$ type crystal structure has been proposed as negative active material, it demonstrates a discharge capacity of up to 970 mAh g^{-1} with a possible reaction mechanism of the Li–M (Cu and Fe) alloy formation–decomposition processes [8]. Other groups also attempt to use transition metal sulfide or phosphide as negative active material [9,10].

On the other hand, the lithium containing Ni, Mn and Co oxide solid solutions have been investigated as positive active materials, but there are a few reports on the solid solutions of transition metal oxides for negative active material applications. We have successfully synthesized some lithium containing Ni, Mn and Co oxide solid solutions such as $Li_xNi_{1/3}Co_{1/3}Mn_{1/3}O_2$, $Li_xNi_{1/2}Co_{1/4}Mn_{1/4}O_2$ and $Li_xNi_{3/5}Co_{1/5}Mn_{1/5}O_2$ for negative active material application [11].

* Corresponding author.

0378-7753/$ – see front matter © 2005 Elsevier B.V. All rights reserved.
doi:10.1016/j.jpowsour.2005.03.206

In this work, the oxide solid solution of nickel oxide and manganese oxide has been newly synthesized, and investigated as a high-capacity negative active material with low cost for lithium secondary cells.

2. Experimental

2.1. Preparation and characterization of active materials

The 3d-transition metal oxides of NiO and Mn_2O_3 were available from High Purity Chemicals Co. Ltd. The oxide solid solution of nickel oxide and manganese oxide was prepared as follows. The precursor compounds of $Ni_{1-a}Mn_aOOH$ with different molar ratios of Ni/Mn were synthesized through a soft chemical process, which was provided by Tanaka Chemical Corp. These compounds were then heated in an electric furnace (Advantec Toyo Kaisha Ltd., KM-1301P) at 150, 350, 600 and 1000 °C in O_2 atmosphere for 16 h, respectively.

The inductively coupled plasma technique (ICP) was used to check composition of the resulting oxide solid solutions; powder X-ray diffraction using Cu Kα radiation was employed to identify the crystalline phase of the materials; the high-resolution X-ray fluorescence spectrometer (HRXRF, Technos, XFRA190) analysis was applied for determining the chemical state of the transition metal.

2.2. Electrochemical test

Electrochemical behavior of transition metal oxide negative electrodes was characterized with constant current charge/discharge test. The electrodes were prepared by coating a paste, which was made of the active material, electrical conductor of acetylene black (AB) and 5 mass% PVdF dissolved in *N*-methyl-2-pyrolidone (NMP) (80:10:10, m/m/m), into/on Al mesh current collector followed by heating at 150 °C under vacuum for 5 h. A three-electrode cell was employed for the electrochemical tests. The metallic lithium was used as the counter and reference electrode. The electrolyte was a mixed solution of EC/DMC/DEC (2/2/1, v/v/v) containing either 1.0 mol dm^{-3} $LiClO_4$. The cell was charged to 0.2 V versus Li/Li^+, then discharged to 3.0 V versus Li/Li^+ at a constant current density of 0.25 mA cm^{-2}. All of the electrochemical tests were carried out in an Ar filled dry box (H_2O: less than 1 ppm) at 25 °C.

3. Results and discussion

3.1. The 3d-transition metal oxides

Electrochemical characteristics of NiO and Mn_2O_3 have been investigated firstly as negative active material. Figs. 1 and 2 represent their charge–discharge characteristics and cycle performance, respectively. It was found that the NiO and Mn_2O_3 show different potential, discharge capacity

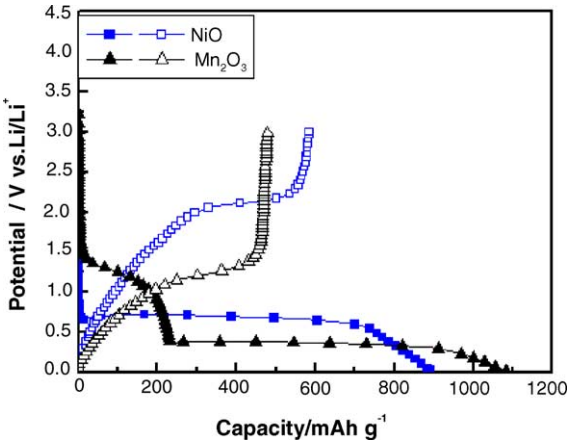

Fig. 1. Charge–discharge characteristics of the NiO and Mn_2O_3 electrodes at 25 °C. The oxide electrodes were charge and discharged at 0.25 mA cm^{-2}.

and cycleability. The NiO is better than Mn_2O_3 on discharge capacity and cycleability, but the Mn_2O_3 shows a lower discharge potential compared with NiO. As a negative material candidate of high-energy density lithium secondary cells, it must have a large capacity and/or lower potential. Therefore, the high-capacity material of nickel oxide and lower potential material of manganese oxide were combined as a solid solution.

3.2. The solid solution of nickel oxide and manganese oxide

In order to obtain a solid solution of nickel oxide and manganese oxide, the $Ni_{1-a}Mn_aOOH$ was selected as precursor compound, the effects of heat-treatment temperature and the composition were investigated. The heat-treatment temperature was decided at 150, 350, 600 and 1000 °C according to the results of TG-DTA measurement (not shown) for $Ni_{1-a}Mn_aOOH$. Fig. 3 shows the typical SEM image change for the $Ni_{0.75}Mn_{0.25}OOH$ heat-treated to different

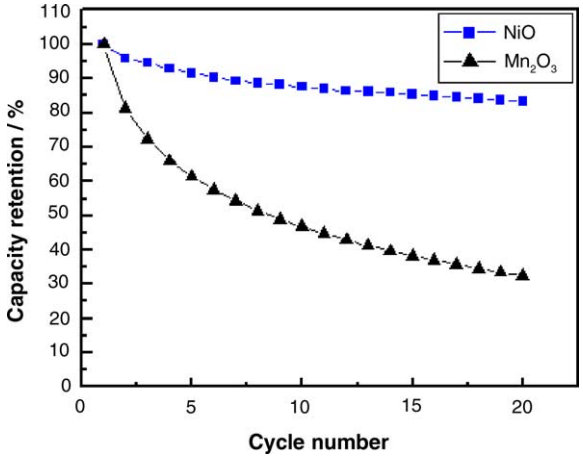

Fig. 2. Comparison of cycleability for NiO and Mn_2O_3. The oxide electrodes were charge and discharged at 0.25 mA cm^{-2}.

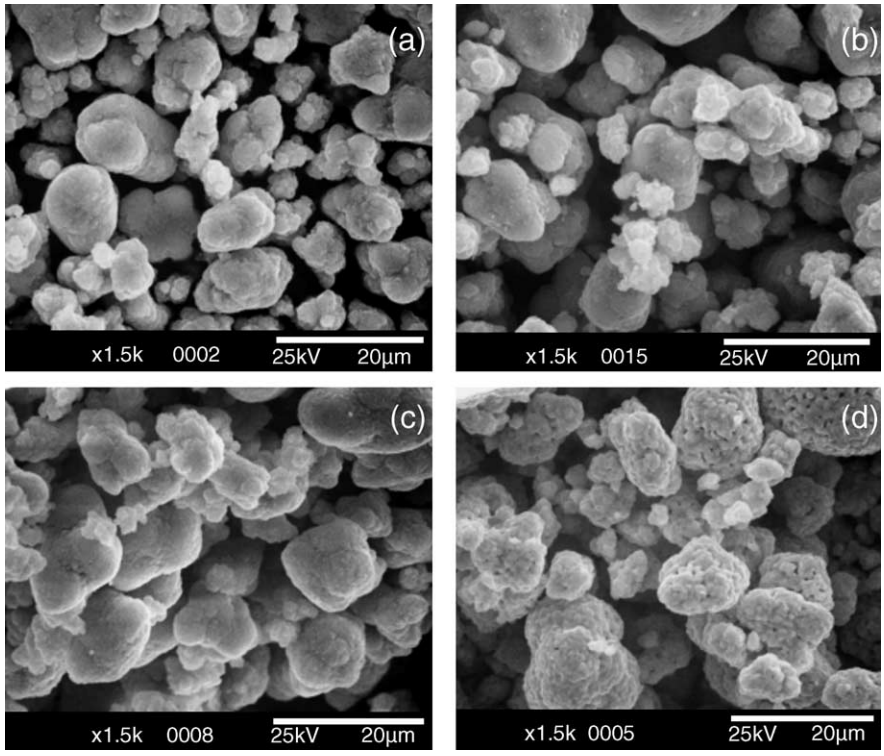

Fig. 3. SEM images of $Ni_{0.75}Mn_{0.25}O_x$ obtained by heating its precursor compound at (a) original state, (b) 350 °C, (c) 600 °C and (d) 1000 °C.

temperatures. There were not notable changes on the morphology and particle size until the temperature up to 600 °C. However, porous particles were obtained at 1000 °C. Table 1 listed the composition and average valence of Ni and Mn in $Ni_{1-a}Mn_aO_x$. The molar content was determined by the ICP analysis and the average valence was calculated based on the oxygen with valence of −2. Fig. 4 shows the XRD patterns of $Ni_{1-a}Mn_aO_x$ for the samples at $a = 0.25$, 0.5 and 0.75 which were heat-treated at 1000 °C. The oxide solid solutions could be assigned as cubic crystal with rock-salt (25 mol% Mn) or spinel structure (50 and 75 mol% Mn), which depends on the Mn content. Fig. 5 shows the effects of heat-treatment temperature on discharge capacity and capacity retention at the 22nd cycle for $Ni_{0.75}Mn_{0.25}O_x$. The discharge capacity was decreased, but cycleability was remarkable improved as increasing heat-treatment temperature until 600 °C. It was considered that the poor cycleability for the solid solution heat-treated at lower temperature was caused by the larger surface area and the H–O bonds existed in the compounds; the smaller capacity for the oxide solid solution obtained

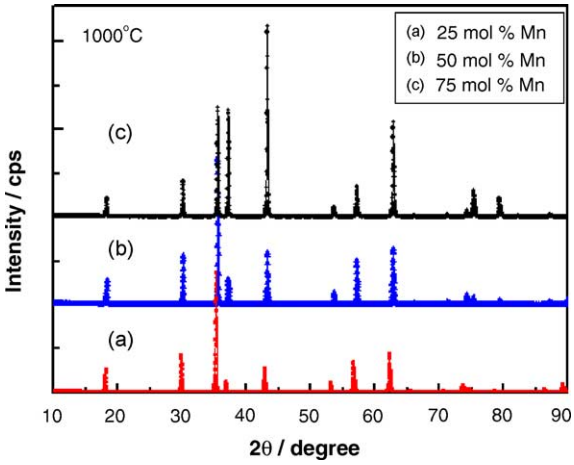

Fig. 4. XRD patterns of (a) $Ni_{0.75}Mn_{0.25}O_x$, (b) $Ni_{0.5}Mn_{0.5}O_x$ and (c) $Ni_{0.25}Mn_{0.75}O_x$. The oxides were obtained by heating their precursor compounds at 1000 °C.

Table 1
Features of Ni–Mn oxyhydroxide and Ni–Mn oxides obtained by heating their precursor compounds at 600 °C

Precursor	Ni/Mn	(Ni + Mn) (wt%)	Product formula	Average valence
NiOOH		78.9	$NiO_{1.28}$	2.56
$Ni_{0.95}Mn_{0.05}OOH$	19/1	79.0	$Ni_{0.95}Mn_{0.05}O_{1.28}$	2.56
$Ni_{0.85}Mn_{0.15}OOH$	17/3	76.8	$Ni_{0.85}Mn_{0.15}O_{1.30}$	2.60
$Ni_{0.75}Mn_{0.25}OOH$	3/1	73.4	$Ni_{0.75}Mn_{0.25}O_{1.36}$	2.72
$Ni_{0.5}Mn_{0.5}OOH$	1/1	71.4	$Ni_{0.5}Mn_{0.5}O_{1.37}$	2.74
$Ni_{0.25}Mn_{0.75}OOH$	3/17	69.7	$Ni_{0.25}Mn_{0.75}O_{1.38}$	2.77

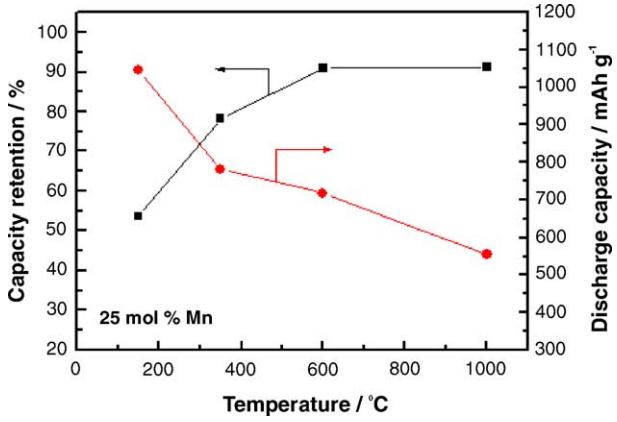

Fig. 5. Effects of heat-treatment temperature on the discharge capacity and capacity retention at 22nd cycle for $Ni_{0.75}Mn_{0.25}O_x$.

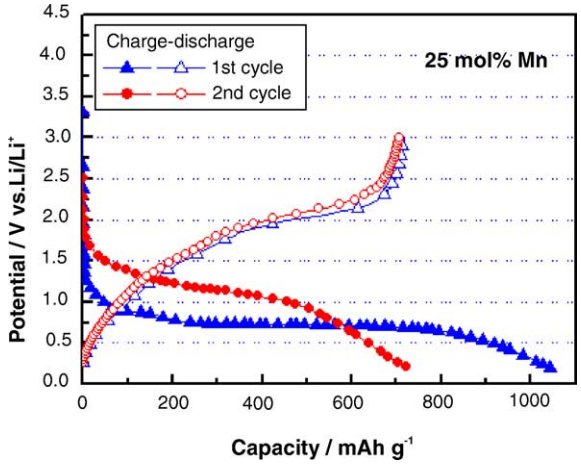

Fig. 6. Charge–discharge characteristics of the Ni and Mn oxide solid solution with 25 mol% Mn. The oxide electrode was charged to 0.20 V and discharged to 3.00 V vs. Li/Li^+ at 0.25 mA cm^{-2}.

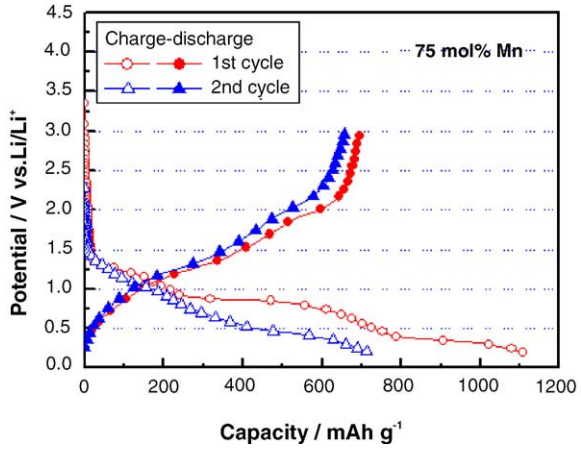

Fig. 7. Charge–discharge characteristics of the Ni and Mn oxide solid solution with 75 mol% Mn. The oxide electrode was charged to 0.20 V and discharged to 3.00 V vs. Li/Li^+ at 0.25 mA cm^{-2}.

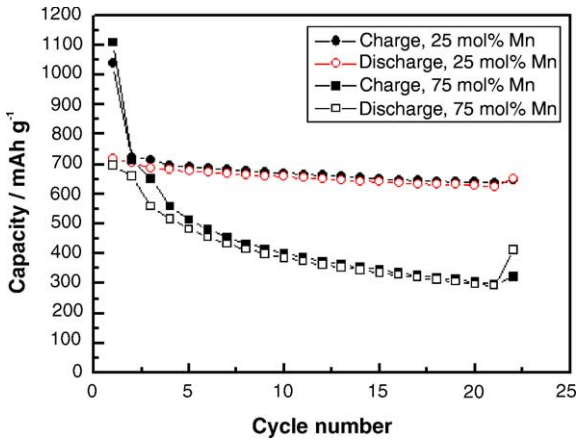

Fig. 8. Comparison of charge–discharge capacity for the Ni and Mn oxide solid solution with 25 and 75 mol% Mn during cycling. The oxide electrodes were charged to 0.20 V and discharged to 3.00 V vs. Li/Li^+ at 0.5 mA cm^{-2}.

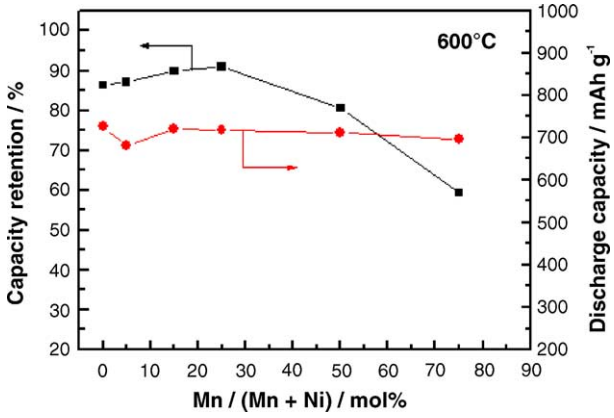

Fig. 9. Change in discharge capacity and capacity retention for the Ni and Mn oxide solid solution with various Mn contents. All of the oxide electrodes were charged to 0.20 V and discharged to 3.00 V vs. Li/Li^+ at 0.5 mA cm^{-2}.

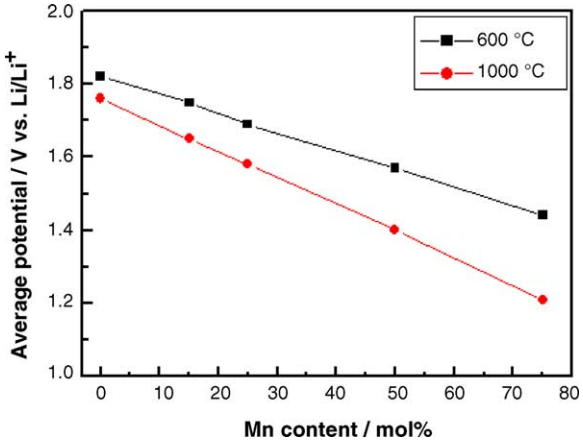

Fig. 10. Change in average discharge potential with Mn content for the Ni and Mn oxide solid solution with various Mn contents.

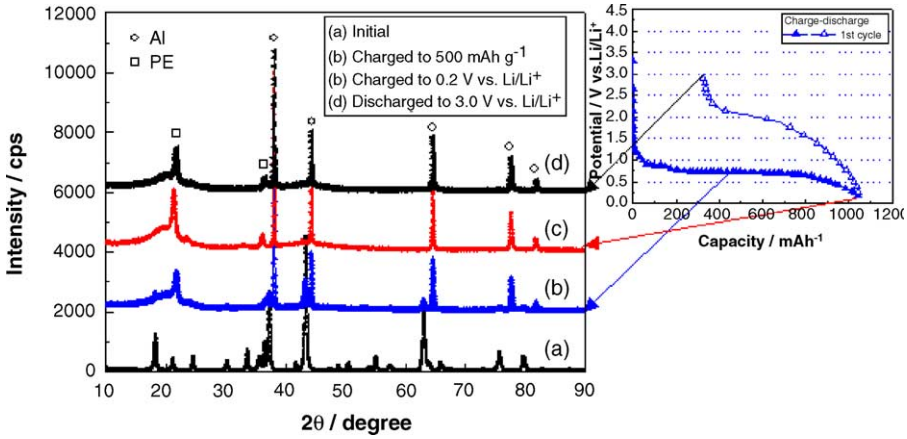

Fig. 11. XRD patterns of $Ni_{0.75}Mn_{0.25}O_{1.36}$ change with different electrochemical treatment.

at high temperature of 1000 °C was caused by the grain growing. Thus, the 600 °C is a suitable heat-treatment temperature for preparing solid solution of nickel oxide and manganese oxide with larger capacity and better cycleability.

Figs. 6 and 7 demonstrate the initial charge–discharge characteristics of $Ni_{0.75}Mn_{0.25}O_{1.36}$ and $Ni_{0.25}Mn_{0.75}O_{1.38}$ obtained by heating their raw materials at 600 °C, respectively. The $Ni_{0.75}Mn_{0.25}O_{1.36}$ and $Ni_{0.25}Mn_{0.75}O_{1.38}$ showed different charge–discharge behavior as negative active materials. Fig. 8 shows the changes in charge–discharge capacity during cycling. A large discharge capacity over 700 mAh g^{-1}, better capacity retention of 91% after 22 cycles and charge–discharge efficiency over 98% was achieved on $Ni_{0.75}Mn_{0.25}O_{1.36}$. In addition, Fig. 9 summarized the dependence of discharge capacity and capacity retention on Mn content for various $Ni_{1-a}Mn_aO_x$ prepared at 600 °C, Fig. 10 describes the average discharge potential change with the Mn content. While increasing Mn content in the compound, the discharge capacity is almost same, but the capacity retention is decreased for the compound with Mn content over 50 mol%, the average discharge potential however shifts towards negative linearly. Nevertheless, the $Ni_{0.75}Mn_{0.25}O_{1.36}$ gave a large discharge capacity, better cycleability and a relatively low average discharge potential among them, thus it was selected as having a better composition.

3.3. Reaction mechanism of $Ni_{0.75}Mn_{0.25}O_{1.36}$ during charge–discharge process

To make the reaction mechanism clear, XRD and HRXRF analysis were carried out for $Ni_{1-a}Mn_aO_x$. According to the XRD results shown in Fig. 11 for the $Ni_{0.75}Mn_{0.25}O_{1.36}$ at different charge–discharge states, it was found that the XRD diffraction peaks become weak and disappeared finally after the deep reduction process, since those oxides became amorphous-like phase or nano-sized particle after the electrochemical reduction. These phenomena were also observed in other transition metal oxides [1].

According to the fitting results of HRXRF, the valences of Ni and Mn at the initial state are ca. 2.0 and 3.7, respectively, after electrochemical reduction to 0.2 V versus Li/Li^+, the Ni^{2+} was reduced to Ni^0, but only a part of Mn^{3+}/Mn^{4+} ion was reduced to metallic Mn. After re-oxidation to 3.00 V versus Li/Li^+, the Mn valence will become 3.0. On the contrary, the Ni will be at a complex chemical state, which needs further fitting. Therefore, the mechanism has been suggested as following reactions:

$$\begin{aligned} &Ni_{1-a}Mn_aO_x + (x - a(1-z) + y)Li^+ + (x - a(1-z) + y)e^- \\ &\quad \rightarrow (1-a)Ni + aMn_z(Mn\text{–}O)_{1-z} + (x - a(1-z))Li_2O \\ &\quad + y\text{Li-polymer} \end{aligned} \tag{2}$$

$$\begin{aligned} &(1-a)Ni + aMn_z(Mn\text{–}O)_{1-z} + y\text{Li-polymer} \\ &\quad + (1 - 0.5a + z - az)Li_2O \Leftrightarrow (1-a)(Ni\text{–}O) \\ &\quad + a/2Mn_2O_3 + (y + 2 - a + 2z - 2az)Li^+ \\ &\quad + \text{polymer} + (y + 2 - a + 2z - 2az)e^- \end{aligned} \tag{3}$$

The electrochemical activity of the transition metal oxide solid solution was caused by the interfacial reaction of lithium on the nano-sized transition metal and their oxides including the polymer phase, and affected by the kind of transition metal and synthesizing conditions, such as temperature and composition. The large irreversible capacity at the first cycle is caused by the irreversible reduction of the oxide especially the Mn ($Mn^{3.7+}$ was reoxidized to Mn^{3+} only), together with polymerization of electrolyte.

4. Conclusions

The $Ni_{1-a}Mn_aO_x$ compounds have been synthesized by heat-treated their precursor compounds of $Ni_{1-a}Mn_aOOH$ solid solutions with various molar ratios of Ni/Mn. It was found that the discharge capacity of nickel and manganese oxide solid solution was decreased with increasing heating temperature. The nickel and manganese oxide

solid solution heated at 600 °C delivered a large discharge capacity around of 700 mAh g^{-1}. Especially, large discharge capacity over 700 mAh g^{-1} with a relatively low average discharge potential of 1.69 V versus Li/Li^+ was achieved on $Ni_{0.75}Mn_{0.25}O_{1.36}$ negative active material. The $Ni_{0.75}Mn_{0.25}O_{1.36}$ gave the best capacity retention of 91% with representative charge–discharge curves even after 22 cycles. The large amount of Mn in the Ni and Mn oxide solid solution caused the poor cycleability.

According to the results of XRD and HRXRF measurements for the oxide solid solution before and after the first charge–discharge, it was clear that the diffraction peaks disappeared after the first charge; all of the nickel and a part of manganese were reduced to metallic state after charge to 0.2 V versus Li/Li^+. It indicates that an amorphous-like or nano-sized phase was formed during the first electrochemical reduction. Therefore, the electrochemical activity of the solid solutions was caused by the interfacial reaction of lithium on the nano-sized transition metal and their oxides, and the large irreversible capacity at the first cycle is caused by the irreversible reduction of the oxide especially the Mn, together with polymerization of electrolyte.

References

[1] P. Poizot, S. Laruelle, S. Grugeon, L. Dupont, J.M. Tarascon, Nature 407 (2000) 496.
[2] P. Poizot, S. Laruelle, S. Grugeon, L. Dupont, J.M. Tarascon, Ionics 6 (3) (2000) 21.
[3] P. Poizot, S. Laruelle, S. Grugeon, L. Dupont, J.M. Tarascon, J. Power Sources 97–98 (2001) 235.
[4] M. Dolle, P. Poizot, L. Dupont, J.M. Tarascon, Electrochem. Solid-State Lett. 5 (2002) A18–A21.
[5] F. Badway, I. Plitz, S. Grugeon, S. Laruelle, M. Dolle, A.S. Gozdz, J.M. Tarascon, Electrochem. Solid-State Lett. 5 (2002) A115–A118.
[6] D. Larcher, G. Sudant, J-B. Leriche, Y. Chabre, J.M. Tarascon, J. Electrochem. Soc. 149 (2002) A234–A241.
[7] S. Grugeon, S. Laruelle, L. Dupont, J.M. Tarascon, Solid State Sci. 5 (2003) 895–904.
[8] S.-K. Chang, H.-J. Kim, S.-T. Hong, J. Power Sources 69–75 (2003) 119–121.
[9] M.N. Obrovac, J.R. Dahn, Electrochem. Solid-State Lett. 5 (2002) A70–A73.
[10] K. Wang, J. Yang, J. Xie, B. Wang, Z. Wen, Electrochem. Commun. 5 (2003) 480.
[11] X. Liu, H. Yasuda, M. Yamachi, The 44th Battery Symposium in Japan, vol. 3A18, Sakai, 2003.